Eurographics Workshop on Visual Computing for Biology and Medicine (2014)
I. Viola, K. Bühler, and T. Ropinski (Editors)

Personalized X-ray Reconstruction of the Proximal Femur via a New Control Point-based 2D-3D Registration and Residual Complexity Minimization

Weimin Yu and Guoyan Zheng

Institute for Surgical Technology and Biomechanics, University of Bern, Switzerland

Abstract

In this paper we present a new control point-based 2D-3D registration approach for a deformable registration of a 3D volumetric template to a limited number of 2D calibrated C-arm images and show its application to a personalized X-ray reconstruction of the proximal femur. In our approach, the 2D-3D registration is done with a hierarchical two-stage strategy: the scaled rigid 2D-3D registration stage followed by a regularized deformable b-spline 2D-3D registration stage. In both stages, a set of control points with uniform spacing are placed over the domain of the 3D volumetric template first. The registrations are then driven by computing updated positions of these control points with intensity-based 2D-2D image registrations of C-arm images with the associated digitally reconstructed radiographs (DRRs), which then allows computing the associated registration transformation at each stage. In order to account for intensity nonstationarities and complex spatially-varying intensity distortion in the deformable b-spline 2D-3D registration stage, the intensity-based 2D-2D image registrations at this stage are done based on minimizing the complexity of the residual images between the C-arm images and the associated DRRs. Comprehensive experiments on simulated images, on images of cadaveric femurs and on clinical datasets are designed and conducted to evaluate the performance of the proposed approach. Quantitative and qualitative evaluation results are given, which demonstrate the efficacy of the present approach.

Categories and Subject Descriptors (according to ACM CCS): I.4.3 [Image Processing and Computer Vision]: Enhancement—Registration

1. Introduction

The applications of registration of a set of two-dimensional (2D) C-arm images with a three-dimensional (3D) volumetric data are pervasive, ranging from pose or morphology determination in image-guided interventions [MTLP12] [ERL*13] to estimation of 3D bone mineral density (BMD) distribution in orthopaedic biomechanics [ARW*10]. The reported techniques for 2D-3D registration can be split into two main categories [MTLP12]: feature-based methods [FL99] [LWH06] [ZGS*09] [BKB*11] and intensity-based methods [ARW*10] [SCT07] [HJ08] [LSW*11] [Zhe11] [WHC*11] [ERL*13]. The methods belonging to the former category typically require an implicit or explicit image segmentation which is error-prone and hard to achieve automatically. The errors in segmentation may lead to errors in the final reconstruction. In contrast, the intensity-based methods directly compare the input X-ray images with the associated simulation images called digitally reconstructed radiographs (DRR), which are obtained by ray casting of a transformed volume data. No segmentation is required.

Depending on whether there exist deformations between the objects imaged by the 2D X-ray images and those imaged by the 3D volumetric intensity data, the methods for achieving intensity-based 2D-3D registration can be classified into two categories: rigid and non-rigid. While intensity-based rigid 2D-3D registration is regarded as a solved problem [MTLP12], intensity-based non-rigid registration is still an active research field [ARW*10] [SCT07] [HJ08] [LSW*11] [Zhe11] [WHC*11] [ERL*13]. Most of these solutions require construction of shape-intensity statistical models.

The contribution of this paper is a new control point-based 2D-3D registration approach for a deformable registration of a 3D volumetric template to a limited number of 2D cali-

DOI: 10.2312/vcbm.20141194

brated C-arm images. Our method does not require construction of shape-intensity statistical mode and uses only one 3D volumetric template. In our method, the 2D-3D registration is done with a hierarchical two-stage strategy: the scaled rigid 2D-3D registration stage followed by a regularized deformable b-spline 2D-3D registration stage. In both stages, a set of control points with uniform spacing are placed over the domain of the 3D volumetric template first. The registrations are then driven by computing updated positions of these control points with intensity-based 2D-2D image registrations of C-arm images with the associated DRRs, which then allows computing the associated registration transformation at each stage. In order to account for intensity non-stationarities and complex spatially-varying intensity distortion in the deformable b-spline 2D-3D registration stage, the intensity-based 2D-2D image registrations at this stage are done based on minimizing the complexity of the residual images between the C-arm images and the associated DRRs.

The paper is organized as follows. Section 2 describes details about our approach. Section 3 presents the experimental results, followed by the conclusions in Section 4.

2. Control Point-based 2D-3D Registration

2.1. Problem formulation

In this work, we assume that we have a set of $Q \geq 2$ C-arm images and that all images are calibrated and co-registered to a common coordinate system called **c**. As we would like to match the 3D volumetric template to the 2D calibrated C-arm images. We consider the 3D volumetric template as the floating image $\mathbf{I}(x_f)$and the 2D calibrated C-arm images as the reference images. The template is aligned to the common coordinate system **c** by following equation:

$$\mathbf{I}(x_{\mathbf{c}}(T_g, T_l)) = \mathbf{I}(T_g \circ T_l \circ x_f) \tag{1}$$

where T_g is a scaled rigid transformation and T_l is a local deformation.

Eq. (1) describes a forward transformation and should be interpreted as follows. Given a voxel x_f in the template, the destination of this voxel under the forward transformation is $x_{\mathbf{c}}(T_g, T_l) = T_g \circ T_l \circ x_f$. The aligned volume at voxel $x_{\mathbf{c}}(T_g, T_l)$ is set to the intensity $\mathbf{I}(x_f)$, which then allows creating DRRs by simulating X-ray projection.

It is suggested by Zheng [Zhe11] that implementing this forward transformation may result in holes in the aligned volume and he suggested that a backward warping as follows should be used.

$$x_f = (T_l)^{-1} \circ ((T_g)^{-1} \circ x_{\mathbf{c}}(T_g, T_l)) \tag{2}$$

It is straightforward to compute the inverse of the scaled rigid transformation T_g. However, it is tricky and time-consuming to compute the inverse of the forward local deformation T_l.

In this paper, we solve the problem differently. The non-rigid registration is done with a hierarchical two-stage strategy: a scaled rigid 2D-3D registration stage (we refer it as "Stage-ScaledRigid2D3D" in the later description) followed by a regularized deformable b-spline 2D-3D registration stage (we refer it as "Stage-Nonrigid2D3D" in the later description). In the first stage, the forward scaled rigid transformation T_g is estimated while in the second stage, we directly estimate $(T_l)^{-1}$, which is a deformation field from the reference image space (i.e., the common coordinate system c) to the floating image space. Obtaining this deformation field will allow us to warp the floating volumetric template to the reference C-arm image space. No inversion of the forward deformation field is required. Details about these two stages will be present below.

2.2. Registration Method

In both stages, a set of control points with uniform spacing are placed over the domain of the volumetric template as follows. Denote the domain of the volumetric template as $\Omega = \{(x,y,z)|0 \leq x \leq n_1, 0 \leq y \leq n_2, 0 \leq z \leq n_3\}$, where n_1, n_2, n_3 denote the number of voxels in x-, y- and z-coordinate direction, respectively. Choosing $s_1, s_2, s_3 \in \Re_{\geq 1}$, describing the spacing (in units of voxels) between any two mesh points (or control points) in each coordinate, a mesh G can be defined by setting:

$$G := s_1 Z_{z_1} \times s_2 Z_{z_2} \times s_3 Z_{z_3} \tag{3}$$

with $z_i := \left\lceil \frac{n_i}{s_i} \right\rceil + 1 \in N$ and $N_{z_i} := \{x \in Z | -1 \leq x \leq z_i\}$.

Such setting guarantees that every voxel of the volumetric template is surrounded by a local mesh cube of size $4 \times 4 \times 4$ due to the fact that a control point is placed in every corner of Ω and an extra layer of control points around Ω is added. There are in total $(z_1+2) \times (z_2+2) \times (z_3+2)$ control points.

2.2.1. Control Point-based 2D-3D Registration Process

In both stages we follow a similar control point-based 2D-3D registration process but with different implementations in some steps, leading to two different 2D-3D registration pipelines. Below we first present this generic 2D-3D registration process, followed by describing the details of different steps in these two different stages.

Step 1: DRR Generation. The generic control point-based 2D-3D registration process starts with generating DRRs using the calibration parameters of the associated input images and the current estimation of the registration transformation. To speed up the DRR generation process,

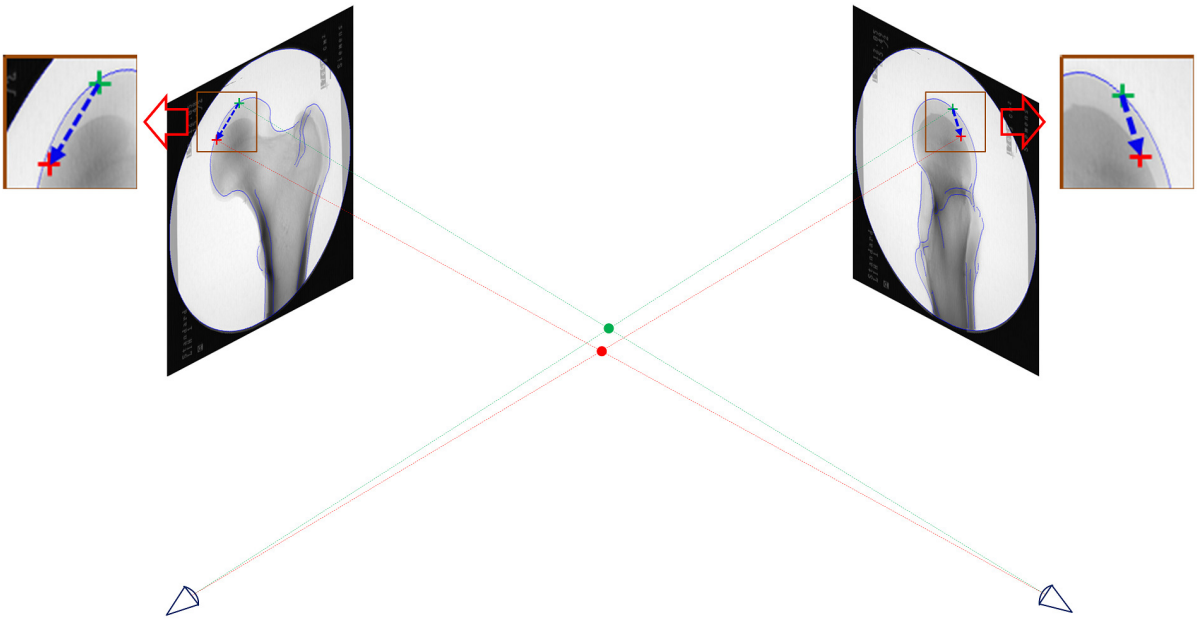

Figure 1: *A schematic view of how to compute paired points for the scaled-rigid registration. Here we focus on only one paired point and the same procedure can be applied to all paired points. On both C-arm images, we superimposed the associated DRRs as well as contours extracted from these DRRs (blue solid lines) for purely visualization purpose. Please note that our 2D-3D registration methods in both stages do not need the extraction of contours from DRRs. The green dot is the original location of a 3D control point and its projection to each DRR is shown as a green cross. A intensity-based 2D-2D image registration is then performed to estimate a 2D similarity transform to update the projection of this control point to a new location (red cross). Using a triangulation-based point reconstruction, we can reconstruct a new 3D location of this control point (red dot) from those updated projection locations (red crosses) to obtain a paired point (green and red dots).*

we have implemented the process in Nvidia's CUDA environment [Apr13].

Step 2: Control Point Projection. Using the current estimation of the registration transformation, we transform all control points from the floating volume space to the reference C-arm image space. To make the description later easier, here we denote the location of an arbitrary control point with index i, j, k as $L^{r,0}_{ijk}$ in the Stage-ScaledRigid2D3D or $L^{n,0}_{ijk}$ in the Stage-Nonrigid2D3D, respectively. After that, using the calibration parameters of the qth C-arm image, we do a forward projection of all transformed control points.

Step 3: 2D-2D Image Registration. In this step, an intensity-based 2D-2D registration between each C-arm image and the associated DRR is performed. Depending on the registration stage, this step is slightly different. Details about the 2D-2D image registration for each stage will be presented below. Common to both stages for this step is that after 2D-2D image registration, locations of all the projected control points in the associated 2D image will be updated using the obtained 2D-2D registration transformation.

Step 4: Triangulation-based Point Reconstruction. Given the updated 2D locations of the projections of a 3D control point with index i, j, k in all images, a updated 3D position of this control point can be reconstructed from those updated 2D locations via triangulation strategy [ZML*02] (see Fig. 1 for an illustration). This is done by minimizing sum of squared distances from this position to all back-projection rays of the corresponding updated 2D locations. Again, depending on the registration stage, we denote the updated position of a control point as $L^{r,1}_{ijk}$ in the Stage-ScaledRigid2D3D or $L^{n,1}_{ijk}$ in the Stage-Nonrigid2D3D, respectively.

Step 5: 2D-3D Registration. Given two point sets with known correspondences, we can compute an updated 2D-3D registration transformation at each stage. Details about how the registration transformation is calculated at each stage will be presented below.

Repeat **Step 1-5** until convergence at each stage to get the final estimation of the 2D-3D registration transformation.

2.2.2. Scaled-rigid 2D-3D Registration Stage

Here, we assume that we have a rough estimation of the initial transformation T^0_g between the floating volume space

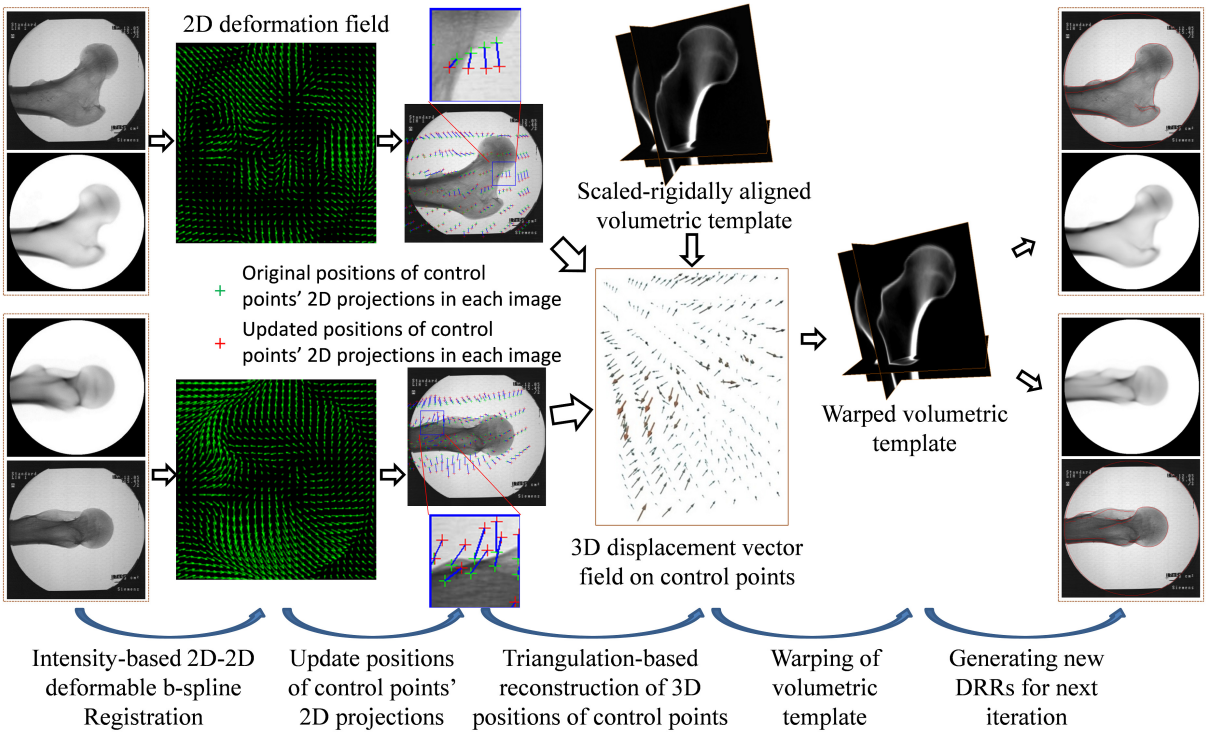

Figure 2: *A schematic view of how the control point-based deformable b-spline 2D-3D registration pipeline is conducted. The complete pipeline consists of following five steps: (1) DRR generation; (2) intensity-based 2D-2D deformable b-spline registration; (3) updating positions of all control points' 2D projections; (4) triangulation-based reconstruction of 3D positions of control points based on the updated positions of the 2D projections; (5) Calculating a displacement vector on each control point and using the resultant 3D displacement field to warp the volumetric template to the reference image space.*

and the reference image space. Given the initial transformation T_g^0, the control point-based scaled rigid 2D-3D registration pipeline will be executed. Below we present the details about how **Step-3** and **Step-5** of this pipeline are performed. All other steps are the same as described in the generic process.

Step 3: 2D-2D Image Registration. At this stage, an intensity-based scaled rigid 2D-2D registration between each 2D DRR to its associated 2D C-arm image is performed using the intensity-based registration toolbox "elastix" [KSM*10] to estimate a similarity transform from each DRR to its associated C-arm image, which will then be used to update the locations of the 2D projections of all control points (See Fig. 1). Please note that at this stage we try to estimate a similarity transform from each DRR to its associated C-arm image and that for the intensity-based scaled rigid 2D-2D registration, we choose to use Mattes mutual information [MHV*03] as the similarity metric and the adaptive stochastic gradient descent optimization [KPSV09] as the optimization method.

Step 5: 3D-3D Scaled-rigid Paired-point Registration. Given two 3D point sets $\{L_{ijk}^{r,0}\}$ and $\{L_{ijk}^{r,1}\}$ with known correspondences, we can compute an updated scaled rigid registration T_g^1.

Step 1 - 5 of the control point-based scaled rigid 2D-3D registration pipeline will be repeated until convergence, and consequently, the output from this stage is the forward transformation T_g.

2.2.3. Regularized Deformable B-spline 2D-3D Registration Stage

The scaled rigid transformation T_g obtained in the last stage allows us to align the floating volume template to the reference image space. After that, the control point-based deformable b-spline 2D-3D registration pipeline will be executed. Fig. 2 shows a schematic view of how the control point-based deformable b-spline 2D-3D registration pipeline is conducted. Below we present the details about how **Step-3** and **Step-5** of this pipeline are performed.

Step 3: 2D-2D Image Registration. Different from the last stage, here we switch the roles of the C-arm images and the DRRs. We propose to conduct an intensity-based de-

formable b-spline 2D-2D registration by minimizing residual complexity [MS10] to match each 2D C-arm image to its associated DRR. The obtained 2D deformation field will be used to update the locations of the 2D projections of all control points (See Fig. 2, where green crosses are the original positions and red crosses are the updated positions). These updated locations will then allow for a triangulation-based reconstruction of new 3D locations of all control points in the next step (**Step 4**). See Fig. 2 for an illustration.

Residual complexity was originally introduced by Myronenko and Song [MS10] as an efficient image similarity measure for handling intensity nonstationarities and complex spatially-varying intensity distortions in mono-modal settings. Considering the inherent differences between a real C-arm image and a simulated DRR, residual complexity will be a better choice than most of the state-of-the-art similarity measures. Assume that the qth C-arm image is I^q_{C-arm} and the associated qth DRR is I^q_{DRR}, we can define the residual complexity S^q_{RC} of these two images as:

$$\begin{cases} r^q = I^q_{C-arm} - I^q_{DRR} \\ c^q = DCT(r^q) \\ S^q_{RC} = \sum \log((c^q)^2/\alpha + 1) \end{cases} \quad (4)$$

where DCT is the forward multidimensional discrete cosine transforms [Str99] and α is a trade-off parameter. Please note that in above equation, I^q_{C-arm}, I^q_{DRR}, and r^q are all in column-vector form.

Step 5: Regularized Deformable B-spline 3D-3D Registration. Given two location sets $\{L^{n,0}_{ijk}\}$ and $\{L^{n,1}_{ijk}\}$ with known correspondences, we can compute a displacement vector $d_{ijk} = L^{n,1}_{ijk} - L^{n,0}_{ijk}$ for every control point (see Fig.2 for an illustration). After that, we can then use the 3D tensor product of the familiar 1D cubic b-splines to compute a free-form deformation at any position of the reference space. For details about how this deformation is computed, we refer to [RSH*99].

Usually the displacement vectors estimated from above procedure are noisy. Regularization is required for a better behavior. In this paper, we propose to regularize the displacement vectors of the control points by minimizing objective function: $E(\mathbf{d}) = \|\Delta\mathbf{d}\|^2$, where $\|\Delta\mathbf{d}\|^2$ is the discrete Laplacian (squared) on the control points with Neumann boundary condition [Str99] and can be efficiently solved with following iterative update:

$$\left|\mathbf{A}^T\mathbf{d}^t\right| = \sqrt{DCT^2(\mathbf{d}^t_x) + DCT^2(\mathbf{d}^t_y) + DCT^2(\mathbf{d}^t_z)}$$
$$\mathbf{d}^{t+1}_l = IDCT\left(\frac{\left|\mathbf{A}^T\mathbf{d}^t\right|}{\left|\mathbf{A}^T\mathbf{d}^t\right| + \gamma\mathbf{B}} \cdot DCT(\mathbf{d}^t_l)\right), \quad for \quad l = x, y, z$$

where $\mathbf{A}$ is a discrete cosine transform basis of the multidimensional Laplacian; DCT and $IDCT$ denote forward and inverse multidimensional discrete cosine transforms; t means the tth iteration; $\mathbf{d}_x, \mathbf{d}_y, \mathbf{d}_z$ are the 3D arrays of corresponding control point displacements. Array $\mathbf{B}$ denotes the eigenvalues of the multidimensional Laplacian with elements: $b_{ijk} = B(i, z_1+2) + B(j, z_2+2) + B(k, z_3+2)$, where $B(n,N) = 2(1 - \cos(\frac{\pi(n-1)}{N}))$. γ is a regularization coefficient.

3. Experiments and Results

We designed and conducted three studies to verify the efficacy of the present method. In all studies the initial transformation T^0_g was estimated by an anatomical landmark-based 2D-3D registration as suggested by Zheng [Zhe11].

Study on simulation data. This study was conducted on CT data of 39 proximal femurs with following procedure. We chose a CT data as the volumetric template and tried to register this template to simulated X-ray images of all other 38 proximal femurs. For each one of these 38 femurs, two simulated X-ray images are generated, one from the anteroposterior (AP) direction and the other from the lateral-medial (LM) direction. Each time, the template was non-rigidly registered to the pair of images. Since the images were generated from a CT data, we can take the CT data as the ground truth to evaluate the 2D-3D registration accuracy. After a semi-automatic segmentation of both datasets, Dice metric (Dice) [Dic45] and surface distance (SD) between the ground truth data and the reconstructed data were calculated. This procedure was repeated 10 times and each time a different CT data was randomly chosen as the volumetric template and matched to the simulated X-ray images of all other 38 proximal femurs, leading to in total $10 \times 38 = 380$ reconstructions. Furthermore, in order to compare the performance of the residual complexity with those of the state-of-the-art similarity measures, we implemented an intensity-based deformable b-spline 2D-2D registration by optimizing Mattes mutual information [MHV*03] in the 2D-2D Image Registration step of the Stage-Nonrigid2D3D while keeping all other conditions the same (Hereafter we refer reconstruction results from this implementation as "MattesMI"). Fig. 3 and Fig. 4 respectively shows the SD and the Dice comparison results when two different similarity measures were used. Overall quantitative comparison results are shown in Table 1. From this table, one can clearly see that better reconstruction results were achieved when the residual complexity was used.

Study on 3 clinical datasets. For this study, we first aligned the CT data of the 39 femurs in the first study to compute a mean intensity model, which was then used as the volumetric template of this study. Each clinical dataset contains two calibrated C-arm images and no ground truth of the imaged patient is available. Thus, we mainly used these datasets to demonstrate qualitatively the performance of the present approach in clinical settings. Fig. 5 shows a patient data reconstruction example

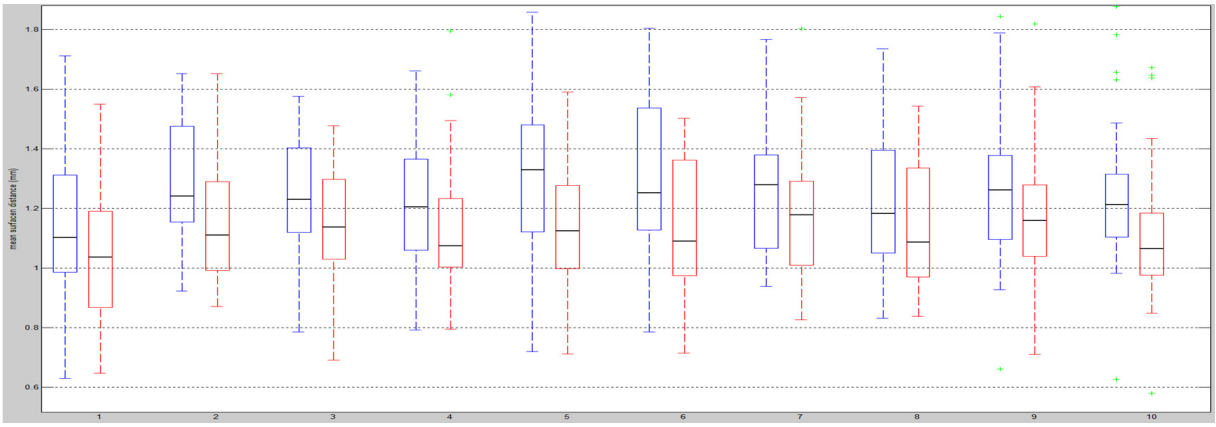

Figure 3: *Box-plots of the surface distances between the reconstructed models and the associated ground truth when 10 different volumetric templates were used with the present method. Blue: results when MattesMI was used, red: results when residual complexity was used.*

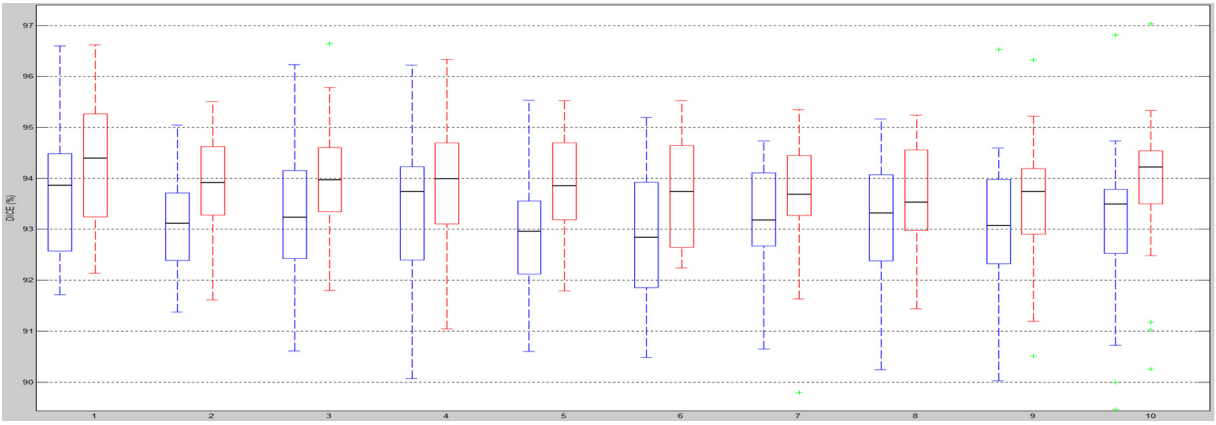

Figure 4: *Box-plots of the Dice coefficients between the reconstructed models and the associated ground truth when 10 different volumetric templates were used with the present method. Blue: results when MattesMI was used, red: results when residual complexity was used.*

Table 1: *Quantitative comparison results when two different similarity measures were used.*

Metrics	Average	Min	Max
When MattesMI was used			
Mean SD (mm)	1.25	0.63	1.93
Mean Dice (%)	93.2	89.5	96.8
When residual complexity was used			
Mean SD (mm)	1.14	0.58	1.82
Mean Dice (%)	93.8	89.8	97.0

Study on calibrated C-arm images of 10 cadaveric femurs. For this study, again we used the mean intensity model created from the CT data of the 39 femurs used in the first study as the volumetric template.The reconstruction accuracies were evaluated by randomly digitizing dozens points from the surface of each femur and then computing the distances from those digitized points to the associated surface model which was segmented from the reconstructed volume. Again, we compared the performance when two different similarity measures were used. When the MattesMI was used, an average mean reconstruction accuracy of 1.4 mm was found. This value decreased to 1.3 mm when the residual complexity was used. Fig.6 shows the errors of reconstructing the 10 cadaveric femurs when the residual complexity was used. It took on average 4 minutes to finish a reconstruction when running on a computer with 2.5 GHz CPU and GPU acceleration.

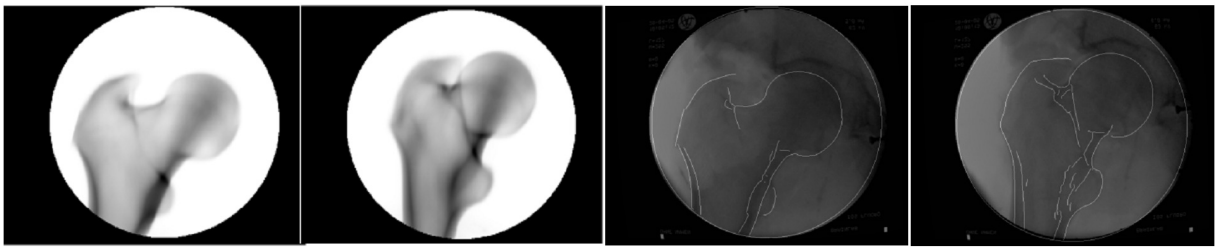

Figure 5: *An example of personalized X-ray reconstruction of the proximal femur from a clinical dataset. Left two images show the projections of the reconstructed volume while the right two images show the original C-arm images superimposed by the contours detected from the top two images.*

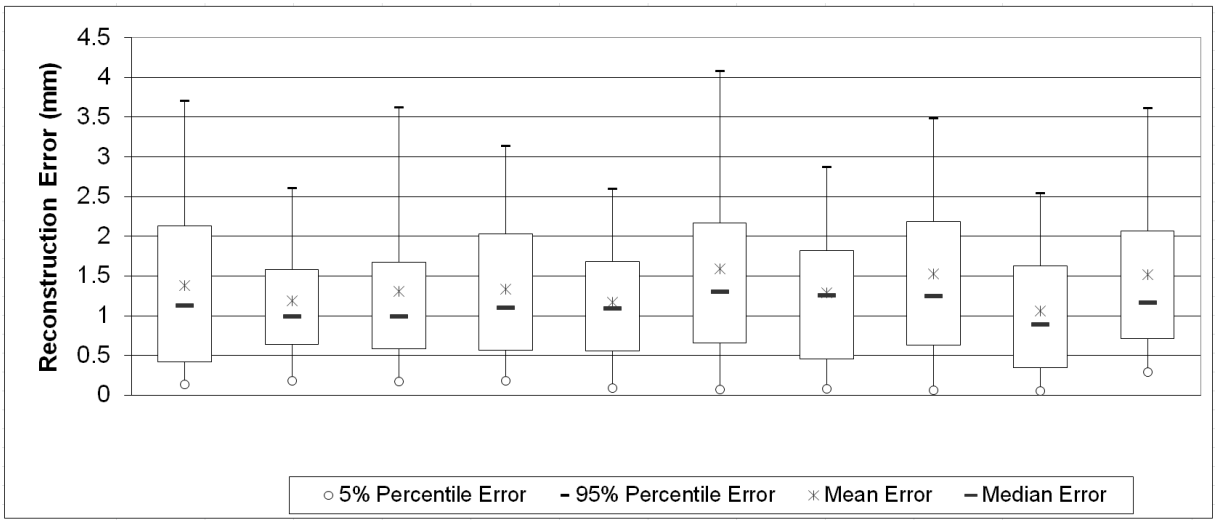

Figure 6: *Box-plots of the errors of reconstructing 10 cadaveric femurs.*

4. Discussions and Conclusions

In this paper, we presented a new approach for the non-rigid registration of a 3D volumetric template to 2D calibrated C-arm images and showed its application to the proximal femur. Unlike other intensity-based non-rigid 2D-3D registration methods, our method does not require construction of shape-intensity statistical models. Additional advantage includes that it can be used to further improve the shape-intensity statistical models-based reconstruction as our method only needs one 3D volumetric template.

Both the method introduced by Zheng [Zhe11] and the present method have been evaluated on the calibrated C-arm images of the 10 cadaveric femurs. An average mean reconstruction accuracy of 1.5 mm was reported in [Zhe11]. In contrast, the present method achieved an average reconstruction accuracy of 1.3 mm. Although further evaluation is needed before we can draw a definitive conclusion, the preliminary evaluation conducted on the calibrated C-arm images of the 10 cadaveric femurs demonstrates that the present method is more accurate than the shape-intensity statistical models-based method introduced by Zheng [Zhe11].

When comparing the performance of the residual complexity with that of Mattes mutual information [MHV*03] on the simulation data, we found a consistent improvement of Dice coefficients and surface distances for all 10 trial as shown in Fig.3. Thus, our experimental results demonstrate that the residual complexity is a better similarity measure than the Mattes mutual information. Our findings are consistent with the results reported in [MS10] where the residual complexity was used for 2D-2D registration or 3D-3D registration tasks. To the authors' best knowledge, this is the first time that the residual complexity was used for 2D-3D registration tasks. The superior performance of the residual complexity over other similarity measures as reported in this paper and in [MS10] can be explained by its ability to account for intensity nonstationarities and complex spatially-varying intensity distortion, as shown by the qualitative evaluation results obtained from the study on 3 clinical datasets (see Fig.5 for an example).

In summary, we developed a new approach for personalized reconstruction of the proximal femur via a new control point-based 2D-3D registration and residual complexity minimization. Studies conducted on simulated data and real data demonstrated the efficacy of the present approach.

5. Acknowledgement

The CT data used in the simulation study was provided by Prof. Dr. P. Zysset. This work was supported by the Swiss National Science Foundation (SNSF) via Project 205321_138009/1 and the Japanese-Swiss Science and Technology Cooperation of the State Secretariat for Education, Research and Innovation (SERI), Switzerland.

References

[Apr13] APRILIS G.: *GPU accelerated volume rendering for use in 2D-3D registration*. Master's thesis, Institute for Surgical Technology and Biomechanics, University of Bern, Switzerland, 2013.

[ARW*10] AHMAD O., RAMAMURTHI K., WILSON K., ENGELKE K., PRINCE R., TAYLOR R.: Volumetric dxa (vxa): A new method to extract 3d information from multiple in vivo dxa images. *Journal BMR 25*, 12 (Dec. 2010), 2744–2751. doi:10.1002/jbmr.140. 1

[BKB*11] BAKA N., KAPTEIN B., BRUIJNE M. D., VAN WALSUM T., GIPHART J., NIESSEN W., LELIEVELDT B.: 2d-3d shape reconstruction of the distal femur from stereo x-ray imaging using statistical shape models. *Med. Image Anal. 15*, 6 (Dec. 2011), 840–850. doi:10.1016/j.media.2011.04.001. 1

[Dic45] DICE L.: Measures of the amount of ecologic association between species. *Ecology 26*, 3 (1945), 297Ű302. doi:doi:10.2307/1932409. 5

[ERL*13] EHLKE M., RAMM H., LAMECKER H., HEGE H.-C., ZACHOW S.: Fast generation of virtual x-ray images for reconstruction of 3d anatomy. *IEEE Trans. Visual. Comput. Graphics 19*, 12 (Dec. 2013), 2673–2682. doi:10.1109/TVCG.2013.159. 1

[FL99] FLEUTE M., LAVALLÉE S.: Nonrigid 3-d/2-d registration of images using statistical models. In *Proc. MICCAI '99* (1999), vol. 1679, pp. 138–147. doi:10.1007/10704282_15. 1

[HJ08] HURVITZ A., JOSKOWICZ L.: Registration of a ct-like atlas to fluoroscopic x-ray images using intensity correspondences. *Int. J. Comput. Assist. Radiol. Surg. 3*, 6 (Dec. 2008), 493–504. doi:10.1007/s11548-008-0264-z. 1

[KPSV09] KLEIN S., PLUIM J., STARING M., VIERGEVER M.: Adaptive stochastic gradient descent optimization for image registration. *INT. J. COMPUT. VISION 81*, 3 (Mar. 2009), 227–239. doi:10.1007/s11263-008-0168-y. 4

[KSM*10] KLEIN S., STARING M., MURPHY K. E., VIERGEVER M., PLUIM J.: Elastix: a toolox for intensity-based medical image registration. *IEEE Trans. Med. Imaging 29*, 1 (Jan. 2010), 196–205. doi:10.1109/TMI.2009.2035616. 4

[LSW*11] LEE O. S. J., SUTTER E., WALL S. J., PRINCE J., TAYLOR R.: Hybrid cone-beam tomographic reconstruction: incorporation of prior anatomical models to compensate for missing data. *IEEE Trans. Med. Imaging 30*, 1 (Jan. 2011), 69–83. doi:10.1109/TMI.2010.2060491. 1

[LWH06] LAMECKER H., WENCKEBACH T., HEDGE H.-C.: Atlas-based 3d-shape reconstruction from x-ray images. In *Proc. ICPR '06* (2006), vol. 1, pp. 371–374. doi:10.1109/ICPR.2006.279. 1

[MHV*03] MATTES D., HAYNOR D., VESSELLE H., LEWELLEN T., EUBANK W.: Pet-ct image registration in the chest using free-form deformation. *IEEE Trans. Med. Imaging 22*, 1 (Jan. 2003), 120–128. doi:10.1109/TMI.2003.809072. 4, 5, 7

[MS10] MYRONENKO A., SONG X.: Intensity-based image registration by minmizing residual complexity. *IEEE Trans. Med. Imaging 29*, 11 (Nov. 2010), 1882–1891. doi:10.1109/TMI.2010.2053043. 5, 7

[MTLP12] MARKELJ P., TOMAZEVIC D., LIKAR B., PERNUS F.: A review of 3d/2d registration methods for image-guided interventions. *Med. Image Anal. 16*, 3 (Apr. 2012), 642–661. doi:10.1016/j.media.2010.03.005. 1

[RSH*99] RUECKERT D., SONODA L., HAYES C., HILL D., LEACH M., HAWKES D.: Nonrigid registration using free-form deformations: application to breast mr images. *IEEE Trans. Med. Imaging 18*, 8 (Aug. 1999), 712–721. doi:10.1109/42.796284. 5

[SCT07] SADOWSKY O., CHINTALAPANI G., TAYLOR R.: Deformable 2d-3d registration of the pelvis with a limited field of view, using shape statistics. In *Proc. MICCAI '07* (2007), vol. 4792, pp. 519–526. doi:10.1007/978-3-540-75759-7_63. 1

[Str99] STRANG G.: The discrete cosine transform. *SIAM Review 41*, 1 (Jan. 1999), 135–147. doi:10.1137/S0036144598336745. 5

[WHC*11] WHITMARSH T., HUMBERT L., CRAENE M. D., BARQUERO L. D. R., FRANGI A.: Reconstructing the 3d shape and bone mineral density distribution of the proximal femur from dual-energy x-ray absorptiometry. *IEEE Trans. Med. Imaging 30*, 12 (Dec. 2011), 2101–2114. doi:10.1109/TMI.2011.2163074. 1

[ZGS*09] ZHENG G., GOLLMER S., SCHUMANN S., DONG X., FEILKAS T., M.A B.: A 2d/3d correspondence building method for reconstruction of a patient-specific 3d bone surface model using point distribution models and calibrated x-ray images. *Med. Image Anal. 13*, 6 (Dec. 2009), 883–899. doi:10.1016/j.media.2008.12.003. 1

[Zhe11] ZHENG G.: Personalized x-ray reconstruction of the proximal femur via intensity-based non-rigid 2d-3d registration. In *Proc. MICCAI '11* (2011), vol. 6892, pp. 598–606. doi:10.1007/978-3-642-23629-7_73. 1, 2, 5, 7

[ZML*02] ZHENG G., MARX A., LANGLOTZ U., WIDMER K., BUTTARO M., NOLTE L.-P.: A hybrid ct-free navigation system for total hip arthroplasty. *Computer assisted surgery 7*, 3 (2002), 129–145. doi:10.1002/igs.10039. 3